# Modeling Multi-Cell IEEE 802.11 WLANs with Application to Channel Assignment

Manoj K. Panda and Anurag Kumar
ECE Department, Indian Institute of Science, Bangalore.
Email: {manoj,anurag}@ece.iisc.ernet.in

***Abstract*—We provide a simple and accurate analytical model for multi-cell IEEE 802.11 WLANs. Our model applies if the *cell radius,* $R$*,* is much smaller than the *carrier sensing range,* $R_{cs}$**. We argue that, the condition** $R_{cs} >> R$ **is likely to hold in a dense deployment of Access Points (APs). We develop a scalable *cell level* model for such WLANs with saturated nodes as well as for TCP-controlled long file downloads. The accuracy of our model is demonstrated by comparison with *ns-2* simulations. Based on the insights provided by our analytical model, we propose a simple channel assignment algorithm which provides *static* assignments that are *Nash equilibria in pure strategies* for the objective of maximizing *normalized network throughput,* and requires only as many steps as there are channels. Furthermore, our channel assignment algorithm does not require any a priori knowledge of topology and can be implemented in a decentralized manner. In contrast to prior work, our approach to channel assignment is based on the *throughput metric*.**

***Index Terms*—throughput modeling, fixed point analysis, channel assignment algorithm, Nash equilibria**

## I. Introduction

This paper is concerned with *infrastructure mode* Wireless Local Area Networks (WLANs) that use the Distributed Coordination Function (DCF) Medium Access Control (MAC) protocol as defined in the IEEE 802.11 standard [1]. Such WLANs contain a number of Access Points (APs). Every client station (STA) in the WLAN associates with exactly one AP. Each AP, along with its associated STAs, defines a *cell*. Thus, in our setting, DCF is used only for *single-hop* communication within the cells, and STAs can access the Internet only through their respective APs. The APs are connected to the Internet by a high-speed wireline local area network. Figure 1 depicts such a *multi-cell* infrastructure WLAN. Each cell operates on a specific channel. Cells that operate on the same channel are called *co-channel*.

To support the ever-increasing user population at high access speeds, WLANs are resorting to dense deployments of APs where, for every STA, there exists an AP close to the STA with which the STA can associate at a high Physical (PHY) rate [2]. However, as the density of APs increases, cell sizes become smaller and, since the number of non-overlapping channels is limited[1], co-channel cells become closer. Nodes in two closely located co-channel cells can suppress each other's transmissions via carrier sensing and interfere with each other's receptions causing packet losses. Clearly, effective planning and management are essential for achieving the benefits of dense deployments of APs. However, large-scale WLANs are difficult to plan and manage since good network engineering models are lacking. In this paper, we first develop an analytical model for multi-cell WLANs and then apply our model to the task of channel assignment.

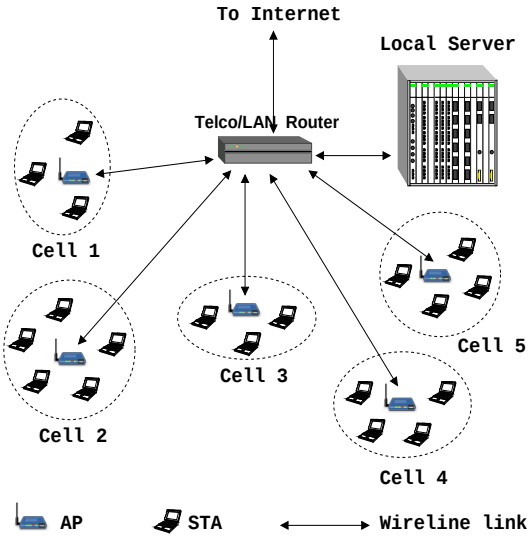


Fig. 1. A multi-cell infrastructure WLAN: DCF is used only for communication within the cells. A high-speed wireline local area network connects the APs to the Internet through a LAN router.

**Our Contributions:** We make the following contributions:

- We develop a scalable *cell level* model for multi-cell WLANs with *arbitrary cell topologies* (Section V).
- We extend the single cell TCP analysis of [3] to multiple interfering cells (Section V-B).
- Based on the insights provided by our analytical model, we propose a simple decentralized algorithm which can provide fast *static* channel assignments (Section VII).

The remainder of this paper is organized as follows. In Section II, we elaborate on our contributions by comparing our work with the existing literature. In Section III, we provide the motivation for our simple cell level model. In Section IV, we provide our network model and summarize our key modeling assumptions. The analytical model is developed in Section V. In Section VI, we validate our model by comparing with *ns-2* simulations. We propose a simple and fast decentralized

This work was supported in part by AirTight Networks, Pune, India, and by the Indo-French Center for the Promotion of Advanced Research (IFCPAR) (Project-4000-IT-A).

[1]For example, the number of non-overlapping channels in 802.11b/g is 3 and that in 802.11a is 12.

channel assignment algorithm in Section VII, and summarize the conclusions in Section VIII. A more detailed version of this paper is available as a technical report [4].

## II. Comparison with Related Literature

Much of the earlier work on modeling WLANs deals with single-AP networks or the so-called *single cells* [5], [6]. Modeling of *multi-hop ad hoc networks* is closely related to that of multi-cell WLANs. In the context of CSMA-based multi-hop packet radio networks, Boorstyn et al. [7] proposed a Markovian model with Poisson packet arrivals and arbitrary packet length distributions. Wang et al. [8], Garetto et al. [9] and Durvy et al. [10] adopted and extended the Boorstyn model to 802.11-based multi-hop ad hoc networks. In the context of multi-cell WLANs, Nguyen et al. [11] proposed a model for dense 802.11 networks assuming all the APs to be operating on the same channel. Bonald et al. [12] proposed to model a multi-cell WLAN as a network of multi-class processor-sharing queues with state-dependent service rates.

Since the activities of each node in a multi-hop ad hoc network (or in a multi-cell WLAN) with general topology evolves over time in a different specific way, one needs to model the network at the *node level* [7], [9], or at the *link level* [8], [10], i.e., the activities of every single node or link and the interactions among them need to be modeled. This requires determining all the *independent sets* of nodes or links and the complexity of the model increases exponentially with the number of nodes or links [13]. We identify a geometric property, which we call the *Pairwise Binary Dependence* (PBD) condition (see A.3 in Section IV), under which multi-cell WLANs can be modeled at the *cell level*. Unlike a node level (resp. link level) model, our cell level model requires determining all the independent sets of *cells*, and thus, the complexity of our model increases with the number of cells rather than nodes (resp. links).

We argue that the PBD condition is likely to hold in a dense deployments of APs, at least approximately. Hence, our cell level model can be applied to obtain a *first-cut* understanding of large-scale WLANs with a dense deployment of APs. Our cell level model is based on the channel contention model of Boorstyn et al. [7] and the transmission attempt model of [6]. Thus, our approach is similar to that of Garetto et al. [9]. However, our model is much simpler than that in [9] (see Discussion 5.1 following Equation 2) and the closed-form expressions for collision probabilities and cell throughputs that we derive are new. We also extend the single cell TCP analysis of [3] to multiple interfering cells (Section V-B).

In [12], MAC contention is modeled by the following heuristic: *the mean time between consecutive packet transmissions correponding to a tagged user is proportional to the number of other contending users plus 1* ("plus 1" accounts for the tagged user). Thus, the mean throughput obtained by a tagged user is inversely proportional to "the number of other contending users plus 1." We show that throughputs cannot be accurately computed based only on the number of contending users (see Observation **O-5** in Section VI).

Channel assignment has been extensively studied (see, e.g., [14], [15], [16], [17], [18] and the references therein). Much of the existing work on channel assignment proposes to minimize the global interference power or maximize the global Signal to Noise and Interference Ratio (SINR) without taking into account the combined effect of the PHY and the MAC layers. Due to carrier sensing, nodes in 802.11 networks get opportunity to transmit for only a fraction of time, and this must be accounted for when computing the global interference power or SINR. Such an approach is found only in [14] where the authors propose to maximize a quantity called "effective channel utilization". In reality, however, end users are more interested in the "throughputs". In contrast to prior work, our approach to channel assignment is based on the *throughput metric* (see Section VII).

## III. Motivation for a Cell Level Model

In a dense deployment of APs with denser user population, it seems practically impossible to apply a node or a link level model for planning and managing the network. However, we can exploit a specific characteristics of dense deployments. Let $R$ denote the *cell radius*, i.e., $R$ is the maximum distance between an AP and the STAs associated to it. Let $R_{cs}$ denote the *carrier sensing range*. We observe that, $R_{cs} >> R$ is likely to hold in a dense deployment of APs where, for every STA, there is an AP very close to the STA. With $R_{cs} >> R$, the network model can be simplified in the following ways:

1) Since any transmitter 'T' is within a small distance $R$ from its receiver 'R', a node 'H' that is beyond a distance $R_{cs}$ from 'T' (i.e., a potential *hidden node*) is unlikely to interfere with 'R'[2], i.e., *carrier sensing would avoid much of the co-channel interference and we may ignore collisions due to hidden nodes*.
2) If Node-1 in Cell-1 can sense the transmissions by Node-2 in Cell-2, then it is likely that all the nodes in Cell-1 can sense the transmissions from all the nodes in Cell-2 and vice versa, i.e., we may assume that *nodes belonging to the same cell have an identical view of the rest of the network and interact with the rest of the network in an identical manner*.

The assumption that the AP and all its associated STAs have an identical view of the network has been applied in a dense AP setting [2] where the authors approximate STA statistics by statistics collected at the APs for efficiently managing their network. We adopt this idea of [2] to develop an analytical model. We identify the locations of the STAs with the locations of their respective APs, and treat a cell as a single entity, thus yielding a scalable *cell level* model. A simple cell level model is particularly suitable for the task of channel assignment since channels are assigned to cells rather than to nodes. At the network planning stage, the locations of the users are not known but the locations of the APs and the expected number of users per cell might be known. Furthermore, much of the

[2]Ignoring noise, we have, SINR $\geq \left(\frac{R_{cs}}{R}\right)^{\nu}$, where $\nu$ is called the *path loss exponent* and takes a value between 2 to 4.

traffic in today's WLANs is downlink, i.e., from the APs to the users, and a large fraction of channel time is occupied by transmissions from the APs. It is then reasonable to develop a model based only on the topology of the APs and the expected number of users per cell, assuming that the users are located close to their respective APs.

## IV. Network Model and Assumptions

We consider scenarios with $R_{cs} >> R$. Based on our discussion in Section III, we assume that simultaneous transmissions by nodes that are farther than $R_{cs}$ from each other result in successful receptions at their respective receivers. We also assume that simultaneous transmissions by nodes that are within $R_{cs}$ always lead to packet losses at their respective receivers, i.e., we ignore the possibility of *packet capture*. We say that two nodes are *dependent* if they are within $R_{cs}$; otherwise, the two nodes are said to be *independent*. Two cells are said to be independent if every node in a cell is independent w.r.t. every node in the other cell; otherwise, the two cells are said to be dependent. Two dependent cells are said to be *completely dependent* if every node in a cell is dependent w.r.t. every node in the other cell. In this broad setting, our key assumptions are the following:

- A.1 Only non-overlapping channels are used.
- A.2 Associations of STAs with APs are static. This implies that the number of STAs in a cell is fixed.
- A.3 **Pairwise Binary Dependence (PBD):** Any pair of cells is either independent or completely dependent.
- A.4 The STAs are so close to their respective APs that packet losses due to channel errors are negligible.

In a dense deployment of APs, due to small cell radius $R$ and $R_{cs} >> R$, two cells would be completely dependent if the corresponding APs lie within $R_{cs}$ of each other and independence would hold beyond $R_{cs}$, i.e., the PBD condition would hold, at least approximately. The PBD condition is a geometric property that enables modeling at the cell level since, *if the PBD condition holds, the relative locations of the nodes within a cell do not matter*. Also, any interferer 'I', which must be within $R_{cs}$ of a receiver 'R', will also be within $R_{cs}$ of the transmitter 'T' if the PBD condition holds. Hence, either (i) 'I' can start transmitting at the same time as 'T' causing *synchronous* collisions at 'R', or (ii) 'I' gets suppressed by T's RTS (or DATA) transmission followed by R's CTS (or ACK) transmission since CTS and ACK frames are given higher priority through SIFS ($<$ DIFS $<$ EIFS). Thus, if the PBD condition holds, nodes do not require deferral by EIFS; deferral by DIFS would suffice. Thus, we assume that contention for medium access always begins after deferral by DIFS and we do not model the impact of EIFS.

## V. Analysis of Multi-Cell WLANs with Arbitrary Cell Topology

In this section, we develop a cell level model for WLANs that satisfy the PBD condition. We provide a generic model and demonstrate the accuracy of our model by comparing with simulations of specific cell topologies pertaining to: (i) networks with linear or hexagonal layout of cells (see Figures 2(a)-2(c)), and (ii) networks with arbitrary layout of cells (see Figure 2(d)). We index the cells by positive integers $1, 2, \ldots, N$, in some arbitrary fashion where $N$ denotes the number of cells. Let $\mathcal{N} = \{1, 2, \ldots, N\}$ denote the set of cells. We form a *contention graph* $\mathcal{G}$ by representing every cell by a vertex and joining every pair of completely dependent cells by an edge. Given the topology of the APs, $\mathcal{G}$ can be obtained.

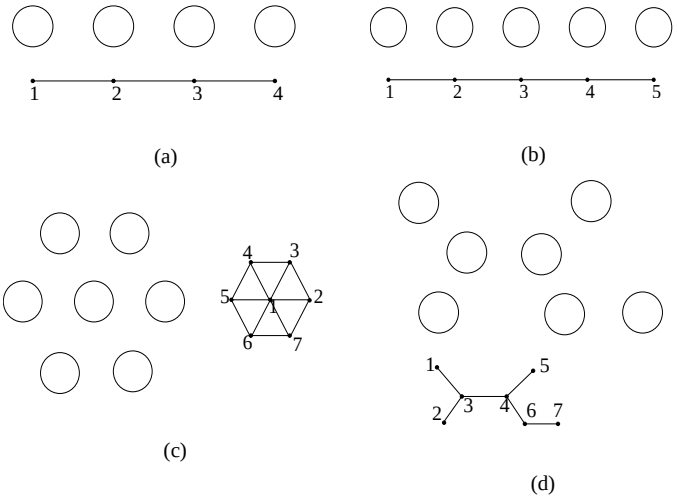


Fig. 2. Examples of multi-cell systems: (a) four linearly placed co-channel cells, (b) five linearly placed co-channel cells, (c) seven hexagonally placed co-channel cells, and (d) seven co-channel cells with an arbitrary cell topology. The co-channel contention graphs have also been shown where the dots represent the cells. Neighbors have been joined by edges. For example (a), the pairs $\{1, 2\}$, $\{2, 3\}$ and $\{3, 4\}$ are dependent and the pairs $\{1, 3\}$, $\{1, 4\}$ and $\{2, 4\}$ are independent.

Let $M$ and $\mathcal{C} = \{1, 2, \ldots, M\}$ denote the number and the set of available channels, respectively. Let $\boldsymbol{c} = (c_1, c_2, \ldots, c_N)$ denote a *channel assignment*, where, $\forall i \in \mathcal{N}$, $c_i \in \mathcal{C}$, denotes the channel assigned to Cell-$i$. Two completely dependent co-channel cells are said to be *neighbors*. Note that, *two completely dependent cells operating on different non-overlapping channels are* ***not*** *neighbors*. Let $\mathcal{N}_i$ $(\subset \mathcal{N})$ denote the set of neighboring cells of Cell-$i$ $(i \in \mathcal{N})$. Note that $i \notin \mathcal{N}_i$. The key to modeling the MAC contention in a multi-cell network, given a channel assignment $\boldsymbol{c}$, is the *co-channel contention graph* $\mathcal{G}(\boldsymbol{c})$ in which only neighbors (i.e., completely dependent co-channel cells) are joined by edges[3]. Figures 2(a)-2(d) also depict the corresponding co-channel contention graphs.

We emphasize that determining a channel assignment $\boldsymbol{c}$ is not part of our analytical model. Given a channel assignment $\boldsymbol{c}$, we can obtain $\mathcal{G}(\boldsymbol{c})$, and our model applies to any $\mathcal{G}(\boldsymbol{c})$. In Section V-A, we model the case where nodes are infinitely backlogged and are transferring packets to one or more nodes in the same cell using UDP connection(s). In Section V-B, we extend to the case when STAs download long files through their respective APs using *persistent* TCP connections.

[3]In particular, with $M = 1$ channel, we have, $\mathcal{G}(\boldsymbol{c}) = \mathcal{G}$.

### A. Modeling with Saturated MAC Queues

Due to the PBD condition, nodes belonging to the same cell have an identical view of the rest of the network. When one node senses the medium idle (resp. busy) so do the other nodes in the same cell and we say that a cell is sensing the medium idle (resp. busy). Since the nodes are saturated, whenever a cell senses the medium idle, all the nodes in the cell decrement their back-off counters per idle back-off slot that elapses in their *local* medium[4] and we say that the cell is in back-off. If the nodes were not saturated, a node with an empty MAC queue would not count down during the "medium idle" periods and the number of *contending* nodes would be time-varying. With saturated AP and STA queues, the number of contending nodes in each cell remains constant.

We say that a cell transmits when one or more nodes in the cell transmit(s). When two or more nodes in the same cell transmit, an *intra-cell* collision occurs. Consider Figure 2(a). There are periods during which all the four cells are in back-off. We model these periods, when none of the cells is transmitting, by the state $\Phi$ where $\Phi$ denotes the *empty set*. The system remains in State $\Phi$ until one or more cell(s) transmit(s). When a cell transmits, its neighbors sense the transmission after a propagation delay and they defer medium access. We then say that the neighbors are *blocked* due to carrier sensing. When a cell is blocked, the back-off counters of all the nodes in the cell are *frozen*. Two neighboring cells can start transmitting together before they could sense each other's transmissions resulting in *synchronous inter-cell* collisions.

We observe that a cell can be in one of the three states: (i) transmitting, (ii) blocked, or (iii) in back-off. Modeling synchronous inter-cell collisions requires a discrete time slotted model. However, this would require a large state space since the cells change their states in an asynchronous manner. For example, consider Figure 2(a) and suppose that Cell-1 starts transmitting and blocks Cell-2 after a propagation delay. However, Cell-3 is independent of Cell-1 and can start transmitting at any instant during Cell-1's transmission. Thus, the evolution of the system is partly asynchronous and partly synchronous. To capture both, we follow a *two-stage* approach along the lines of [9]. In the first stage, we ignore inter-cell collisions and assume that blocking due to carrier sensing is immediate. We develop a continuous time model as in [7] to obtain the fraction of *time* each cell is transmitting/blocked/in back-off. In the second stage, we obtain the fraction of *slots* in which various subsets of neighboring cells can start transmitting together. This would allow us to compute the collision probabilities accounting for synchronous inter-cell collisions. We combine the above through a fixed-point equation and compute the throughputs using the solution of the fixed-point equation.

We define the following as in [6]:

$\beta_i :=$ (transmission) attempt probability (over the back-off slots) of the nodes in Cell-$i$

$\gamma_i :=$ collision probability as seen by the nodes in Cell-$i$ (conditioned on an attempt being made)

The attempt probability $\beta_i$ of the nodes in Cell-$i$, $\forall i \in \mathcal{N}$, can be related to $\gamma_i$ by (see [6])

$$\beta_i = \frac{1 + \gamma_i \ldots + \gamma_i^K}{b_0 + \gamma_i b_1 \ldots + \gamma_i^k b_k + \ldots + \gamma_i^K b_K} \tag{1}$$

where $K$ denotes the *retry limit* and $b_k$, $0 \leq k \leq K$, denotes the mean back-off sampled after $k$ collisions.

**The First Stage:** When Cell-$i$ and some (or all) of its neighboring cells are in back-off they contend until one of the cells, say, Cell-$j$, $j \in \mathcal{N}_i \cup \{i\}$, starts transmiting. Since, we ignore inter-cell collisions in the first stage, the possibility of two or more neighboring cells starting transmission together is ruled out. When Cell-$i$ starts transmitting, we say that it has become *active*. When Cell-$i$ becomes active, it gains control over its local medium by *immediately* blocking its neighbors that are not yet blocked. We assume that the time until Cell-$i$ goes from the back-off state to the active state is exponentially distributed with mean $\frac{1}{\lambda_i}$. The activation rate $\lambda_i$ is given by

$$\lambda_i = \frac{1 - (1 - \beta_i)^{n_i}}{\sigma} \tag{2}$$

where $n_i$ denotes the number of nodes in Cell-$i$, $\sigma$ denotes the duration of a back-off slot (in seconds) and $1 - (1 - \beta_i)^{n_i}$ is the probability that there is an attempt in Cell-$i$ per back-off slot. Notice that we have converted the aggregate attempt probability in a cell per (discrete) back-off *slot* to an attempt rate over (continuous) back-off *time*. Also notice that, our assumption of "exponential time until transition from the back-off state to the active state" is the continuous time analogue of the assumption of "geometric number of slots until attempt" in the discrete time model of [6].

*Discussion 5.1:* In [9], the authors use an unconditional activation rate $\lambda$ over all times as well as a conditional activation rate $g$ over the back-off times and relate the two rates through a throughput equation which makes their model complicated. We use a single activation rate $\lambda$ which is conditional on being in the back-off state and our model is much simpler than that of [9]. ■

When Cell-$i$ becomes active, its neighboring cells remain blocked (due to Cell-$i$) until Cell-$i$'s transmission finishes and an idle DIFS period elapses. When Cell-$i$ becomes active through a successful transmission (resp. an intra-cell collision) its neighbors remain blocked for a *success time* $T_s$ (resp. a *collision time* $T_c$)[5]. The active periods of Cell-$i$ are of mean duration $\frac{1}{\mu_i}$ given by

$$\begin{aligned} \frac{1}{\mu_i} &= \left( \frac{n_i \beta_i (1-\beta_i)^{n_i - 1}}{1 - (1-\beta_i)^{n_i}} \right) \cdot (T_s) \\ &\quad + \left( 1 - \frac{n_i \beta_i (1-\beta_i)^{n_i - 1}}{1 - (1-\beta_i)^{n_i}} \right) \cdot (T_c) \end{aligned} \tag{3}$$

[4]Nodes belonging to different cells, in general, have different views of the network activity.

[5]For the *Basic Access* (resp. *RTS/CTS*) mechanism, $T_s$ corresponds to the time DATA-SIFS-ACK-DIFS (resp. RTS-SIFS-CTS-SIFS-DATA-SIFS-ACK-DIFS) and $T_c$ corresponds to the time DATA-DIFS (resp. RTS-DIFS).

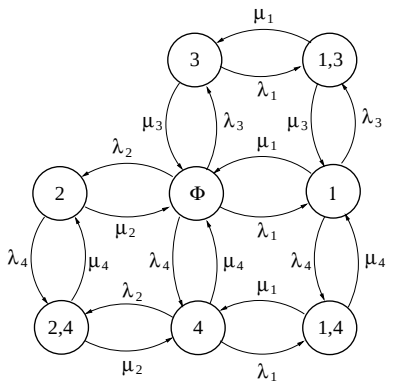


Fig. 3. The CTMC describing the cell level contention for the four linearly placed cells given in Figure 2(a).

where $\frac{n_i\beta_i(1-\beta_i)^{n_i-1}}{1-(1-\beta_i)^{n_i}}$ is the probability that Cell-$i$ becomes active through a success given that it becomes active. It is worthwhile now to mention the *insensitivity* result of Boorstyn et al. [7] which says that the product-form solution provided by their model is insensitive to the packet length distribution and depends only on the mean packet lengths. Applying their insensitivity argument, we take the active periods of Cell-$i$ to be i.i.d. exponential random variables with mean $\frac{1}{\mu_i}$.

Due to carrier sensing, at any point of time, only a set $\mathcal{A}$ ($\subset \mathcal{N}$) of mutually independent cells can be active together, i.e., $\mathcal{A}$ must be an *independent set* (of vertices) of $\mathcal{G}(\boldsymbol{c})$. From $\mathcal{G}(\boldsymbol{c})$, we can determine the set of cells $\mathcal{B}_{\mathcal{A}}$ that get blocked due to $\mathcal{A}$, and the set of cells $\mathcal{U}_{\mathcal{A}}$ that remain in back-off, i.e., the set of cells in which nodes can continue to decrement their back-off counters. Note that $\mathcal{A}$, $\mathcal{B}_{\mathcal{A}}$ and $\mathcal{U}_{\mathcal{A}}$ form a partition of $\mathcal{N}$. *We take $\mathcal{A}(t)$, i.e., the set $\mathcal{A}$ of active cells at time $t$, as the state of the multi-cell system at time $t$*. Due to exponential activation rates and active periods, at any time $t$, the rate of transition to the next state is completely determined by the current state $\mathcal{A}(t)$. For example, Cell-$j$, $j \in \mathcal{U}_{\mathcal{A}}$, joins the set $\mathcal{A}$ (and its neighboring cells that are also in $\mathcal{U}_{\mathcal{A}}$ join the set $\mathcal{B}_{\mathcal{A}}$) at a rate $\lambda_j$. Similarly, Cell-$i$, $i \in \mathcal{A}$, leaves the set $\mathcal{A}$ (and its neighboring cells that are blocked only due to Cell-$i$ leave the set $\mathcal{B}_{\mathcal{A}}$) to join the set $\mathcal{U}_{\mathcal{A}}$ at a rate $\mu_i$. In summary, *the process $\{\mathcal{A}(t), t \geq 0\}$ has the structure of a Continuous Time Markov Chain (CTMC)*. This CTMC contains a finite number of states and is irreducible. Hence, it is stationary and ergodic. The set of all possible independent sets which constitutes the state space of the CTMC $\{\mathcal{A}(t), t \geq 0\}$ is denoted by $\boldsymbol{\mathcal{A}}$. For a given contention graph, $\boldsymbol{\mathcal{A}}$ can be determined. For the topology given in Figure 2(a), we have $\mathcal{N} = \{1, 2, 3, 4\}$ and $\boldsymbol{\mathcal{A}} = \{\Phi, \{1\}, \{2\}, \{3\}, \{4\}, \{1, 3\}, \{1, 4\}, \{2, 4\}\}$ where we recall that $\Phi$ denotes the empty set. The CTMC $\{\mathcal{A}(t), t \geq 0\}$ corresponding to this example is given in Figure 3.

It can be checked that the transition structure of the CTMC $\{\mathcal{A}(t), t \geq 0\}$ satisfies the Kolmogorov Criterion for reversibility (see [19]). Hence, the stationary probability distribution $\pi(\mathcal{A}), \mathcal{A} \in \boldsymbol{\mathcal{A}}$, satisfies the detailed balance equations,

$$\pi(\mathcal{A})\lambda_i = \pi(\mathcal{A} \cup \{i\})\mu_i \ , \ (\forall i \in \mathcal{U}_{\mathcal{A}})$$

and the stationary probability distribution has the form

$$\pi(\mathcal{A}) = \left(\prod_{i \in \mathcal{A}} \rho_i\right) \pi(\Phi), \quad (\forall \mathcal{A} \in \boldsymbol{\mathcal{A}}) \tag{4}$$

where $\rho_i := \frac{\lambda_i}{\mu_i}$ and $\pi(\Phi)$ (which denotes the stationary probability that none of the cells is active) is determined from the normalization equation

$$\sum_{\mathcal{A} \in \boldsymbol{\mathcal{A}}} \pi(\mathcal{A}) = 1. \tag{5}$$

Combining Equations 4 and 5, we obtain

$$\pi(\mathcal{A}) = \frac{\left(\prod_{i \in \mathcal{A}} \rho_i\right)}{\sum_{\mathcal{A} \in \boldsymbol{\mathcal{A}}} \left(\prod_{j \in \mathcal{A}} \rho_j\right)} \quad (\forall \mathcal{A} \in \boldsymbol{\mathcal{A}}). \tag{6}$$

*Convention:* A product $\prod$ over an empty index set is taken to be equal to 1.

**The Second Stage:** We now compute the collision probabilities $\gamma_i$'s accounting for inter-cell collisions. Note that $\gamma_i$ is conditional on an attempt being made by a node in Cell-$i$. Hence, to compute $\gamma_i$, we focus only on those states in which Cell-$i$ can attempt. Clearly, Cell-$i$ can attempt in State-$\mathcal{A}$ iff it is in back-off in State-$\mathcal{A}$, i.e., iff $i \in \mathcal{U}_{\mathcal{A}}$. In all such states a node in Cell-$i$ can incur intra-cell collisions due the other nodes in Cell-$i$. Furthermore, some (or all) of Cell-$i$'s neighbors might also be in back-off in State-$\mathcal{A}$. If a neighboring cell, say, Cell-$j$, $j \in \mathcal{N}_i$, is also in back-off in State-$\mathcal{A}$, i.e., if $j \in \mathcal{U}_{\mathcal{A}}$, then a node in Cell-$i$ can incur inter-cell collisions due to the nodes in Cell-$j$. The collision probability $\gamma_i$ is then given by Equation 7 (appears at the top of the next page). A formal derivation of Equation 7 can be found in Appendix A of [4].

**Fixed Point Formulation:** Equations 2, 3, 6, 7 and $\rho_i := \frac{\lambda_i}{\mu_i}$ can express the $\gamma_i$'s as functions of only the $\beta_i$'s. Together with Equation 1, they yield an $N$-dimensional fixed point equation where we recall that $N$ is the total number of cells. In all of the cases that we have considered, the fixed point iterations were observed to converge to the same solutions irrespective of starting points. However, we have not yet been able to analytically prove the uniqueness of solutions.

**Calculating the Throughputs:** The stationary probabilities of the CTMC $\{\mathcal{A}(t), t \geq 0\}$ can provide the fraction of time $x_i$ for which Cell-$i$ is *unblocked*. A cell is said to be unblocked when it belongs to either $\mathcal{A}$ or $\mathcal{U}_{\mathcal{A}}$. Thus, $\forall i \in \mathcal{N}$,

$$x_i = \sum_{\mathcal{A} \in \boldsymbol{\mathcal{A}} \,:\, i \in \mathcal{A} \cup \mathcal{U}_{\mathcal{A}}} \pi(\mathcal{A}). \tag{8}$$

*Definition 5.1:* Let $\mathcal{G}^i(\boldsymbol{c})$, $i \in \mathcal{N}$, denote the subgraph obtained by removing Cell-$i$ and its neighboring cells in $\mathcal{N}_i$ from $\mathcal{G}(\boldsymbol{c})$. For a given $\mathcal{G}(\boldsymbol{c})$, let $\Delta$ be defined as follows:

$$\Delta := \sum_{\mathcal{A} \in \boldsymbol{\mathcal{A}}} \left(\prod_{j \in \mathcal{A}} \rho_j\right) \tag{9}$$

$$\gamma_i = \frac{\sum_{\mathcal{A}\in\boldsymbol{\mathcal{A}}\,:\,i\in\mathcal{U}_{\mathcal{A}}} \pi(\mathcal{A}) \left[1-(1-\beta_i)^{n_i-1}\prod_{j\in\mathcal{N}_i\,:\,j\in\mathcal{U}_{\mathcal{A}}}(1-\beta_j)^{n_j}\right]}{\sum_{\mathcal{A}\in\boldsymbol{\mathcal{A}}\,:\,i\in\mathcal{U}_{\mathcal{A}}} \pi(\mathcal{A})} \qquad (\forall i\in\mathcal{N}) \tag{7}$$

Let $\Delta_i$ denote the $\Delta$ corresponding to the subgraph $\mathcal{G}^i(\boldsymbol{c})$. ■

An important observation which facilitates the computation of the $x_i$'s is given by the following theorem.

*Theorem 5.1:* The fraction of time $x_i$ for which Cell-$i$ is unblocked is given by

$$x_i = \frac{(1+\rho_i)\Delta_i}{\Delta}, \quad \forall i\in\mathcal{N}. \tag{10}$$

*Proof:* See Appendix B of [4]. ■

Let $\Theta_i$ denote the aggregate throughput of Cell-$i$ in a given multi-cell network and let $\Theta_{n_i,singlecell}$ denote the aggregate throughput of Cell-$i$ if it was an isolated cell containing $n_i$ nodes. Both $\Theta_i$ and $\Theta_{n_i,singlecell}$ are in packets/sec. We approximate $\Theta_i$ by

$$\Theta_i \quad = \quad x_i \cdot \Theta_{n_i,singlecell} \tag{11}$$

and $\Theta_i$ divided by $n_i$ gives the per node throughput $\theta_i$ in Cell-$i$, i.e., $\theta_i = \frac{\Theta_i}{n_i}$ (packets/sec).

*Discussion 5.2:* Equation 11 is justified as follows. If Cell-$i$ is indeed an isolated cell, then we have $x_i = 1$ and $\Theta_i = \Theta_{n_i,singlecell}$. However, in general, Cell-$i$ remains unblocked only for a fraction of time $x_i$. If we ignore the time wasted in inter-cell collisions, the times during which Cell-$i$ is unblocked would consist only of the back-off slots and the activities of Cell-$i$ by itself. Thus, we approximate the aggregate throughput of Cell-$i$, over the times during which it is unblocked, by $\Theta_{n_i,singlecell}$ and $\Theta_{n_i,singlecell}$ multiplied with $x_i$ gives the aggregate throughput $\Theta_i$ of Cell-$i$ in the multi-cell network. Clearly, Equation 11 is an approximation since the time wasted in inter-cell collisions have been ignored. However, (1) it is quite accurate when compared with the simulations (see Section VI), and (2) it allows efficient computation of throughputs since $\Theta_{n_i,singlecell}$ can be obtained from a single cell analysis and the $\Delta$ as well as the $\Delta_i$'s can be computed using efficient algorithms [13]. ■

**Large $\rho$ Regime:** Let $\eta$ (resp. $\eta_i$) denote the number of Maximum Independent Sets (MISs) of $\mathcal{G}(\boldsymbol{c})$ (resp. $\mathcal{G}^i(\boldsymbol{c})$) (see Definition 5.1). Notice that, $\eta_i$ is also equal to the number of MISs of $\mathcal{G}(\boldsymbol{c})$ to which Cell-$i$ belongs. From Equation 6 it is easy to see that, as $\rho_i\to\infty$, $\forall i\in\mathcal{N}$, we have,

$$\pi(\mathcal{A}) \to \begin{cases} \frac{1}{\eta} & \text{if } \mathcal{A} \text{ is an MIS,} \\ 0 & \text{otherwise.} \end{cases}$$

i.e., only an MIS of cells can be active at any point of time. Also, from Equations 6, 8, 9 and 10, we observe that, as $\rho_i\to\infty$, $\forall i\in\mathcal{N}$, we have,

$$x_i \to \frac{\eta_i}{\eta}\ ,$$

where we recall that $x_i$ is the fraction of time for which Cell-$i$ is unblocked. The quantity

$$x_i = \frac{\Theta_i}{\Theta_{n_i,singlecell}}$$

can be interpreted as the throughput of Cell-$i$, normalized with respect to Cell-$i$'s single cell throughput. Thus, a cell which belongs to every MIS of $\mathcal{G}(\boldsymbol{c})$ (resp. does not belong to any MIS of $\mathcal{G}(\boldsymbol{c})$) obtains a normalized throughput 1 (resp. 0). Similar observations have been made in [8] for link throughputs. Defining the *normalized network throughput* $\bar{\Theta}$ by

$$\bar{\Theta} := \sum_{i=1}^{N} x_i\ , \tag{12}$$

and recalling that an MIS of $\mathcal{G}(\boldsymbol{c})$ is active at any point of time, we further observe that, as $\rho_i\to\infty$ for all $i\in\mathcal{N}$, we have,

$$\bar{\Theta} \to \alpha(\mathcal{G}(\boldsymbol{c}))\ ,$$

where $\alpha(G)$ denotes the cardinality of an MIS (of vertices) in a graph $G$ and is also called the *independence number* of $G$. Notice that, $\alpha(G)$ is a measure of *spatial reuse* in a network with contention graph $G$, and thus, $\alpha(\mathcal{G}(\boldsymbol{c}))$ is a measure of spatial reuse induced by the assignment $\boldsymbol{c}$.

### B. Extension to TCP Traffic

Our extension to TCP-controlled long file downloads is based on the single cell TCP-WLAN interaction model of [3]. The model proposed in [3] has been shown to be quite accurate when: (1) the TCP server is connected to the AP by a high-speed wireline LAN such that the AP in the WLAN is the bottleneck, (2) every STA has a *single persistent* TCP connection, (3) there are no packet losses due to buffer overflow, (4) the TCP timeouts are set large enough to avoid timeout expirations due to Round Trip Time (RTT) fluctuations, and (5) the delayed ACK mechanism is disabled. We keep the above assumptions in this paper.

In [3], the authors propose to model a single cell having an AP and an arbitrary number of STAs with long-lived TCP connections by an "equivalent saturated network" which consists of a saturated AP and a single saturated STA. "This equivalent saturated model greatly simplifies the modeling problem since the TCP flow control mechanisms are now implicitly hidden and the total throughput can be computed using the saturation analysis [3]." Using the equivalent saturated model of [3], the analysis of Section V-A can be applied to TCP-controlled long file downloads, taking $n_i = 2, \forall i\in\mathcal{N}$.

## VI. Results and Discussion

We carried out simulations using *ns-2.31* [20]. We created the example topologies given in Figure 2(a)-2(d) by setting the cell radii and the distances among the cells such that the PBD condition holds. Nodes were randomly placed within the cells. The saturated case was simulated with high rate CBR

TABLE I
RESULTS FOR THE FOUR LINEARLY PLACED CELLS GIVEN IN FIGURE 2(A) WHEN EACH CELL CONTAINS $n = 5$ NODES

| Cell index | $\gamma_{sim}$ | $\gamma_{ana}$ | $\theta_{sim}$ (pkts/sec) | $\theta_{ana}$ (pkts/sec) | $\theta_{\infty}$ (pkts/sec) |
|---|---|---|---|---|---|
| 1 | 0.2351 | 0.2399 | 94.48 | 97.41 | 93.53 |
| 2 | 0.3005 | 0.3146 | 41.21 | 46.66 | 46.76 |
| 3 | 0.2999 | 0.3146 | 41.66 | 46.66 | 46.76 |
| 4 | 0.2359 | 0.2399 | 93.99 | 97.41 | 93.53 |

TABLE II
RESULTS FOR THE FIVE LINEARLY PLACED CELLS GIVEN IN FIGURE 2(B) WHEN EACH CELL CONTAINS $n = 5$ NODES

| Cell index | $\gamma_{sim}$ | $\gamma_{ana}$ | $\theta_{sim}$ (pkts/sec) | $\theta_{ana}$ (pkts/sec) | $\theta_{\infty}$ (pkts/sec) |
|---|---|---|---|---|---|
| 1 | 0.1882 | 0.1897 | 129.35 | 131.35 | 140.29 |
| 2 | 0.3321 | 0.3975 | 8.69 | 8.64 | 0 |
| 3 | 0.1892 | 0.1925 | 123.35 | 126.41 | 140.29 |
| 4 | 0.3321 | 0.3975 | 8.72 | 8.64 | 0 |
| 5 | 0.1884 | 0.1897 | 129.31 | 131.35 | 140.29 |

TABLE III
RESULTS FOR THE SEVEN ARBITRARILY PLACED CELLS GIVEN IN FIGURE 2(D) WHEN CELL-$i$, $1 \leq i \leq 7$ CONTAINS $n_i = i + 1$ NODES

| Cell index $i$ | $n_i$ | $\gamma_{sim}$ | $\gamma_{ana}$ | $\theta_{sim}$ (pkts/sec) | $\theta_{ana}$ (pkts/sec) | $\theta_{\infty}$ (pkts/sec) |
|---|---|---|---|---|---|---|
| 1 | 2 | 0.0669 | 0.0666 | 320.66 | 325.26 | 349.94 |
| 2 | 3 | 0.1163 | 0.1163 | 216.19 | 219.65 | 236.09 |
| 3 | 4 | 0.2764 | 0.3280 | 12.48 | 12.97 | 0 |
| 4 | 5 | 0.3105 | 0.3318 | 34.29 | 40.20 | 46.76 |
| 5 | 6 | 0.2505 | 0.2585 | 83.77 | 84.92 | 77.26 |
| 6 | 7 | 0.3574 | 0.3787 | 28.67 | 32.40 | 32.81 |
| 7 | 8 | 0.3062 | 0.3139 | 56.87 | 59.21 | 56.90 |

over UDP connections. For the TCP case, we created one TCP download connection per STA. Each TCP connection was fed by an FTP source with the TCP source agent attached directly to the AP to emulate a local server. The AP buffer was set large enough to avoid buffer losses. The EIFS deferral and the delayed ACK mechanism were disabled. Each case was simulated 20 times, each run for 200 sec of "simulated time". We took 11 Mbps data rate and packet payloads of 1000 bytes.

We computed the single cell throughputs for the saturated case as in [6] and that for the TCP case as in [3]. The single cell throughputs thus obtained from known analytical models and the $x_i$'s computed by our multi-cell model were plugged into Equation 11 to obtain cell throughputs in the multi-cell scenarios. The function "*fsolve()*" of MATLAB was used for solving the $N$-dimensional fixed point equation. We report the results for "Basic Access". Similar results were obtained with "RTS/CTS". We do not report the results for the hexagonal topology given in Figure 2(c) which can be found in [4]. In the following, quantities denoted with a subscript "*sim*" (resp. "*ana*") correspond to results obtained from *ns-2* simulations (resp. fixed point analysis). In each case, $\theta_{\infty}$ represents the throughput per-node obtained by taking $\rho_i \to \infty, \forall i \in \mathcal{N}$.

### A. Results for the Saturated Case

Tables I and II summarize the results for the example multi-cell cases depicted in Figures 2(a) and 2(b), respectively, when each cell contains $n = 5$ saturated nodes. Table III summarizes the results for the example case given in Figure 2(d) when

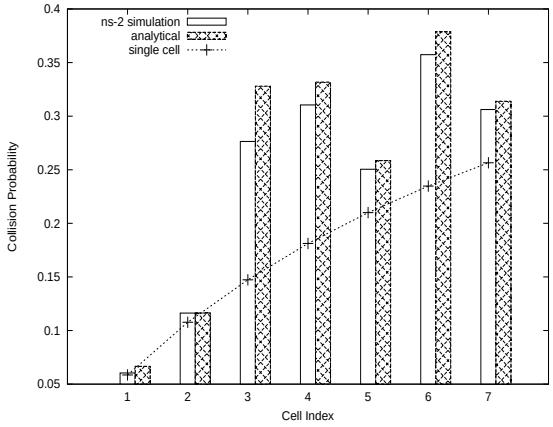


Fig. 4. Comparing collision probability $\gamma$ for the scenario in Figure 2(d) when Cell-$i$, $1 \leq i \leq 7$, contains $n_i = i + 1$ saturated nodes.

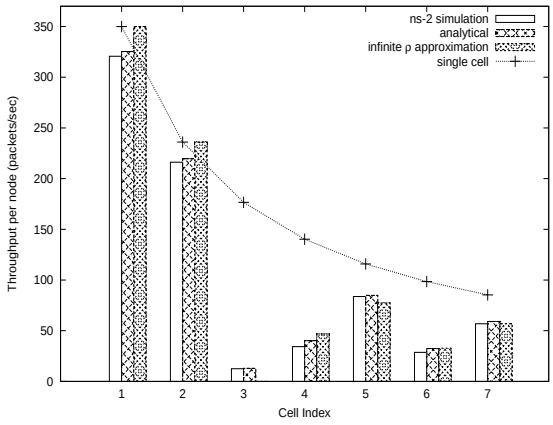


Fig. 5. Comparing throughput per node $\theta$ for the scenario in Figure 2(d) when Cell-$i$, $1 \leq i \leq 7$, contains $n_i = i + 1$ saturated nodes.

Cell-$i$, $1 \leq i \leq 7$, contains $n_i = i + 1$ saturated nodes. We show the plots corresponding to Table III in Figures 4 and 5 which compare the collision probability $\gamma$ and the throughput per node $\theta$, respectively. In Figures 4 and 5, we also show the relevant single cell results, i.e., the results one would expect had the seven cells been mutually independent. Referring Tables I-III, and Figures 4 and 5, we make the following observations:

**O-1.)** Collision probabilities (resp. throughputs) in the multi-cell scenarios are always higher (resp. lower) than the corresponding single cell values (see Figures 4 and 5) because (a) inter-cell collisions can be significant, and (b) due to blocking, cells get opportunity to transmit only a fraction of time.

**O-2.)** Our analytical model is quite accurate (less than 10% error in most cases) in predicting the collision probabilities and throughputs. The throughput predictions with $\rho_i \to \infty, \forall i \in \mathcal{N}$, is fairly accurate but the fixed point analysis provides more accurate predictions. Furthermore, our model works well with either equal or unequal number of nodes per cell.

**O-3.)** Our analytical model always over-estimates the throughputs since the time wasted in inter-cell collisions have been ignored. Ignoring inter-cell collisions in the first stage of the

TABLE IV
RESULTS FOR THE AP CORRESPONDING TO FIGURE 2(A) WHEN EACH CELL CONTAINS 1 AP AND $n = 5$ STAS

| Cell index | $\gamma_{sim,AP}$ | $\gamma_{ana,AP}$ | $\theta_{sim,AP}$ (pkts/sec) | $\theta_{ana,AP}$ (pkts/sec) | $\theta_{\infty,AP}$ (pkts/sec) |
|---|---|---|---|---|---|
| 1 | 0.1038 | 0.1033 | 306.33 | 318.73 | 304.35 |
| 2 | 0.1560 | 0.1574 | 153.16 | 169.18 | 152.18 |
| 3 | 0.1555 | 0.1574 | 153.06 | 169.18 | 152.18 |
| 4 | 0.1038 | 0.1033 | 306.41 | 318.73 | 304.35 |

TABLE V
RESULTS FOR THE AP CORRESPONDING TO FIGURE 2(B) WHEN EACH CELL CONTAINS 1 AP AND $n = 5$ STAS

| Cell index | $\gamma_{sim,AP}$ | $\gamma_{ana,AP}$ | $\theta_{sim,AP}$ (pkts/sec) | $\theta_{ana,AP}$ (pkts/sec) | $\theta_{\infty,AP}$ (pkts/sec) |
|---|---|---|---|---|---|
| 1 | 0.0728 | 0.0775 | 381.21 | 387.16 | 456.53 |
| 2 | 0.1793 | 0.1950 | 75.16 | 85.62 | 0 |
| 3 | 0.0744 | 0.0832 | 340.24 | 346.47 | 456.53 |
| 4 | 0.1786 | 0.1950 | 75.23 | 85.62 | 0 |
| 5 | 0.0728 | 0.0775 | 381.15 | 387.16 | 456.53 |

TABLE VI
RESULTS FOR THE AP CORRESPONDING TO FIGURE 2(D) WHEN EACH CELL CONTAINS 1 AP AND $n = 5$ STAS

| Cell index | $\gamma_{sim,AP}$ | $\gamma_{ana,AP}$ | $\theta_{sim,AP}$ (pkts/sec) | $\theta_{ana,AP}$ (pkts/sec) | $\theta_{\infty,AP}$ (pkts/sec) |
|---|---|---|---|---|---|
| 1 | 0.0610 | 0.0670 | 421.70 | 425.83 | 456.53 |
| 2 | 0.0604 | 0.0670 | 421.92 | 425.83 | 456.53 |
| 3 | 0.2010 | 0.2528 | 33.79 | 38.50 | 0 |
| 4 | 0.1561 | 0.1685 | 141.80 | 156.41 | 152.18 |
| 5 | 0.0987 | 0.1028 | 317.39 | 329.06 | 304.35 |
| 6 | 0.1551 | 0.1644 | 158.55 | 172.64 | 152.18 |
| 7 | 0.1061 | 0.1099 | 301.15 | 314.10 | 304.35 |

model also over-estimates the fraction of time spent in back-off. Thus, the collision probabilities are also over-estimated. However, had we not accounted for the inter-cell collisions in the second stage, our analytical collision probabilities would have been equal to the corresponding single cell collision probabilities (see Figures 4 and 5).

**O-4.)** Throughput distribution among the cells can be very unfair even over long periods of time. Furthermore, introduction of a new co-channel cell can drastically alter the throughput distributions. For example, compare Tables I and II. Cell-2 and Cell-4 severely get blocked if Cell-5 is introduced to the four cell network given in Figure 2(a).

**O-5.)** The throughput of a cell cannot be accurately determined based only on the *number* of interfering cells. Consider, for example, Figure 2(d). Cell-3 and Cell-4 each have two neighbors but their per node throughputs $\theta$ are quite different (see Figure 5). In particular, $\theta_4 > \theta_3$ even though $n_3 = 4 < n_4 = 5$. This is due to Cell-7 which blocks Cell-6 for certain fraction of time during which Cell-4 gets opportunity to transmit whereas Cell-1 and Cell-2 are almost never blocked and Cell-3 is almost always blocked due to Cell-1 and Cell-2. Thus, *topology plays the key role and heuristic methods based only on the number of neighbors would fail.*

### *B. Results for the TCP Download Case*

Tables IV-VI summarize the AP statistics for the topologies in Figures 2(a), 2(b) and 2(d), respectively. We show the plots corresponding to Table VI in Figures 6 and 7 which compare

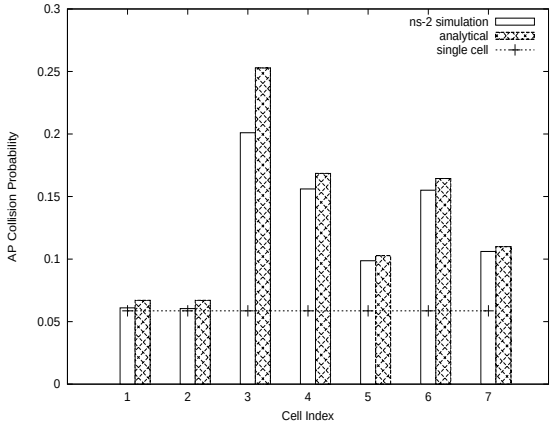


Fig. 6. Comparing collision probability $\gamma$ for the scenario in Figure 2(d) when each cell contains an AP and $n = 5$ STAs.

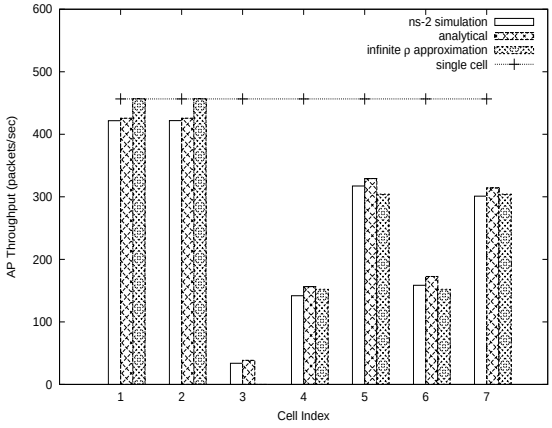


Fig. 7. Comparing throughput per node $\theta$ for the scenario in Figure 2(d) when each cell contains an AP and $n = 5$ STAs.

the collision probability $\gamma$ and the throughput per node $\theta$, respectively. Referring Tables IV-VI, and Figures 6 and 7, we conclude that the foregoing observations (**O.1**-**O.5**) for the saturated case carry over to TCP-controlled long file transfers as well. Referring Tables IV-VI we extend the validity of the equivalent saturated model of [3] as follows:

**O-6.)** The equivalent saturated model of [3] proposed in the context of a single cell, preserves its desirable properties, i.e., it predicts the AP statistics quite well when extended to a multi-cell WLAN that satisfies the PBD condition.

### *C. Variation with $\rho$*

Clearly, the $\rho_i$'s are functions of the $\beta_i$'s and the payload size. The $\beta_i$'s cannot be preset to desired values since they are determined by the back-off adaptation mechanism of DCF. Thus, we study the effect of variation of $\rho$ by varying the payload size. Figures 8 and 9 depict the variation with payload size of analytically computed collision probabilities and normalized cell throughputs, respectively, for the seven cell network of Figure 2(d) when each cell contains $n = 10$ saturated nodes. Similar results were obtained for the TCP case as well. From Figures 8 and 9, we observe that:

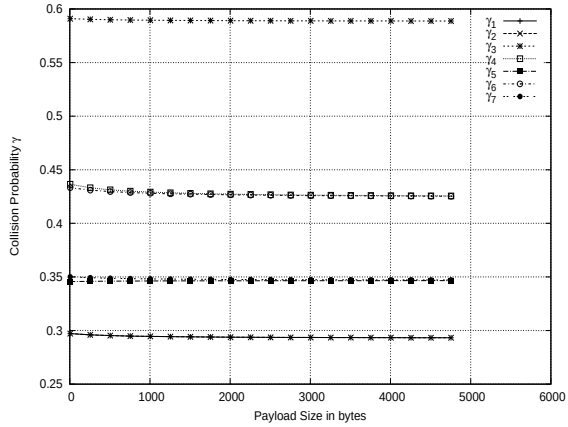


Fig. 8. Variation of collision probabilities with payload size for the seven cell network in Figure 2(d).

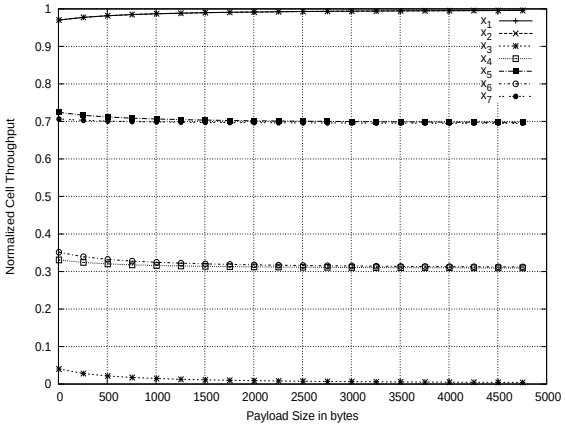


Fig. 9. Variation of normalized cell throughputs with payload size for the seven cell network in Figure 2(d).

**O-7.)** The results are largely insensitive to the variation in payload size. Moreover, the normalized cell throughputs are approximately equal to the normalized throughputs obtained by taking $\rho_i \rightarrow \infty$, $1 \leq i \leq 7$, i.e., we have, $x_1 = x_2 \approx 1, x_3 \approx 0, x_4 \approx x_6 \approx \frac{1}{3}, x_5 \approx x_7 \approx \frac{2}{3}$. Hence, we may assume that, $\bar{\Theta} \approx \alpha(\mathcal{G}(\boldsymbol{c}))$ for all values of $\rho$.

## VII. A Simple and Fast Channel Assignment Algorithm for Maximizing $\bar{\Theta}$

Any channel assignment algorithm requires a means to evaluate the *goodness* of an assignment based on which it determines a *better* assignment. Our analytical model can provide such feedback. In fact, we could apply our model in conjunction with the Linear Reward-Inaction ($L_{R-I}$) algorithm [21]. However, we found the $L_{R-I}$ algorithm to be extremely slow (see [4] for the details). The Linear Reward-Penalty ($L_{R-P}$) algorithm of [17] and the *simulated annealing* algorithm of [18] guarantee convergence to a globally optimum solution as the number of iterations goes to infinity. A *greedy* version of simulated annealing algorithm in [18] converges relatively fast but still takes a large number of iterations to converge. Moreover, the $L_{R-I}$ algorithm and the greedy simulated annealing algorithm can only provide channel assignments that are *Nash equilibria in pure strategies* in the sense that changing the channel of one of the cells does not increase the expected *utility*.

Suppose that our objective is to maximize the normalized network throughput $\bar{\Theta}$ (see Equation 12). As discussed in Observation **O-7**, $\bar{\Theta} \approx \alpha(\mathcal{G}(\boldsymbol{c}))$. Hence, maximizing $\alpha(\mathcal{G}(\boldsymbol{c}))$ would maximize $\bar{\Theta}$. Thus, we need to determine an assignment $\boldsymbol{c}$ to transform $\mathcal{G}$ to $\mathcal{G}(\boldsymbol{c})$ so that $\alpha(\mathcal{G}(\boldsymbol{c}))$ is maximized. To this end, we propose the following channel assignment algorithm. (recall that $M$ denotes the number of available channels)

**Maximal Independent Set Algorithm (mISA) :**

1. Begin with $\mathcal{G}$ (since we have not yet assigned channels).
2. Choose a *maximal* independent set (mIS)[6] of cells in $\mathcal{G}$, assign them Channel-1, and then remove them from $\mathcal{G}$.
3. Increment the channel index and repeat Step-2 above on the *residual* graph until exactly one channel is left.
4. Assign Channel-$M$ to all the cells in the residual graph after $M-1$ steps.

Notice that mISA takes only $M$ steps. Clearly, mISA is based on a classical graph coloring technique, but the novelty lies in our recognizing the notion of optimality that mISA provides which is given by the following theorem.

*Theorem 7.1:* The channel assignments by mISA are Nash equilibria in pure strategies for the objective of maximizing normalized network throughput $\bar{\Theta}$ as $\rho_i \rightarrow \infty$, $\forall i \in \mathcal{N}$.

*Proof:* Note that the residual graph may become *null* (i.e., it might not have any vertices left) after $M' < M$ steps. If the residual graph becomes null in less than $M$ steps, then every cell would have a channel different from that of all its neighbors and, we have, $\bar{\Theta} = N$, i.e., mISA would provide a globally optimum solution and we are done. Hence, assume that the residual graph after $M-1$ steps is not null.

Suppose that $N_j$ cells are assigned Channel-$j$ in Step-$j$, $1 \leq j \leq M-1$. Let $\mathcal{G}_j$ be the residual graph after $j$ steps, $1 \leq j \leq M-1$. Let $\bar{\Theta}_k$ denote the aggregate normalized throughput of the cells on Channel-$k$, $1 \leq k \leq M$. Then, we have, $\bar{\Theta}_j = N_j$, $1 \leq j \leq M-1$, due to independence, and $\bar{\Theta}_M = \alpha(\mathcal{G}_{M-1})$. Hence, $\bar{\Theta} = \sum_{k=1}^{M} \bar{\Theta}_k = \sum_{j=1}^{M-1} N_j + \alpha(\mathcal{G}_{M-1})$. Suppose that a cell on Channel-$j$, $j \neq M$, is moved to Channel-$k$, $k \neq j$. Then, $\bar{\Theta}_j$ decreases by 1 but $\bar{\Theta}_k$ can increase by at most 1. Hence, $\bar{\Theta}$ cannot increase. Suppose now that a cell on Channel-$M$ is moved to Channel-$j$, $1 \leq j \leq M-1$. Clearly, any cell on Channel-$M$ is dependent (in the original graph $\mathcal{G}$) w.r.t. at least one of the $N_j$ cells on Channel-$j$ since the $N_j$ cells that were already on Channel-$j$, $1 \leq j \leq M-1$, form an mIS. Hence, $\bar{\Theta}_j$ does not change but $\bar{\Theta}_M$ can only decrease. Hence, $\bar{\Theta}$ cannot increase by changing the channel of *only* one of the cells and the theorem is proved. ■

**Implementation of mISA:** mISA can be implemented in a decentralized manner as follows. APs sample random back-offs using a contention window $W$ and contend for accessing the medium using Channel-1. If $W$ is chosen large enough,

[6]The lower case 'm' corresponds to "maximal" as opposed to the upper case 'M' which corresponds to "maximum".

the probability that two or more neighboring APs sample the same back-off would be small. When an AP wins the contention it keeps transmitting broadcast packets separated by SIFS for some duration $T >> \sigma W$ where we recall that $\sigma$ is the duration of a back-off slot. This emulates the infinite $\rho$ situation since an AP after wining the contention does not relinquish control over its local medium, and its neighboring APs remain blocked for the duration $T$. We had observed that, as $\rho_i \to \infty$, $\forall i \in \mathcal{N}$, only the cells that belong to an MIS obtain non-zero normalized throughputs. But this holds only in an *ensemble average* sense. If an AP, after wining the contention, does not relinquish control over its local medium, in a particular *sample path*, an mIS of APs (which may not be an MIS) would *grab* the channel during $T$. This is not surprising since with infinite $\rho_i$'s, the CTMC $\{\mathcal{A}(t), t \geq 0\}$ becomes absorbing with the maximal independent sets of cells as the absorbing states and we cannot expect the time average to be equal to the ensemble average.

At time $T$, APs that could transmit consecutive broadcast packets stop contending until time $(M-1) \times T$ and APs that remain blocked switch to Channel-2, sample fresh back-offs and keep contending until $2T$ and so on. APs that remain blocked throughout the duration $(M-1) \times T$ stick to Channel-$M$. Thus, in every time duration $T$, a maximal independent set of APs would be assigned a channel. Normal network operation can begin after time $(M-1) \times T$. Notice that, *mISA does not require any knowledge of AP topology and runs in a completely decentralized manner without any message passing*. In addition, if there is a central controller to which the APs can communicate, mISA can be repeated several times before normal network operation could begin. The central controller, which obtains the global view of the channel assignments, can choose the best among the solutions provided by mISA. In absence of centralized control, mISA can be invoked periodically. Thus, mISA can be easily implemented in real networks in a completely decentralized manner if the number of channels for all APs is the same and known. However, mISA requires loose synchronization among the APs similar to the channel assignment algorithms in [17] and [18].

## VIII. Conclusions and Future Work

In this paper, we identified a Pairwise Binary Dependence (PBD) condition that allows a scalable cell level modeling of WLANs. The PBD condition is likely to hold at higher PHY rates and dense AP deployments. We developed a cell level model both under saturation condition and for TCP-controlled long file downloads. Our analytical model was shown to be quite accurate and insightful. Thus, we believe that our modeling framework is a significant step toward gaining "first-cut" analytical understanding of WLANs with dense deployments of APs. Based on the insights provided by our model, we also proposed a simple decentralized algorithm called mISA which can provide channel assignments that are Nash equilibria in pure strategies in only as many steps as there are channels. Although mISA is based on a standard graph coloring technique, we have formally established the notion of optimality which mISA provides (i.e., Nash equilibria in pure strategies) and the conditions under which the optimality is attained (i.e., when $\rho_i \to \infty, \forall i \in \mathcal{N}$). We also discussed how mISA can be implemented in real networks. Developing simple and practical algorithms for general objective functions, other than maximizing the normalized network throughput, is a topic of our ongoing research. Also, developing simple and accurate analytical models for TCP-controlled short file transfers is an important topic which we plan to address in the future.

## References


[1] "Wireless LAN Medium Access Control (MAC) and (PHY) Layer Specifications, ANSI/IEEE Std 802.11, 1999 Edition."

[2] R. Murty, J. Padhye, R. Chandra, A. Wolman, and B. Zill, "Designing High Performance Enterprise Wi-Fi Networks," in *5th USENIX Symposium on Networked Systems Design and Implementation NSDI'08*, 2008.

[3] R. Bruno, M. Conti, and E. Gregori, "An accurate closed-form formula for the throughput of long-lived TCP connections in IEEE 802.11 WLANs," *Computer Networks*, vol. 52, pp. 199–212, 2008.

[4] M. K. Panda and A. Kumar, "Modeling Multi-Cell IEEE 802.11 WLANs with Application to Channel Assignment," Indian Institute of Science, Tech. Rep., 2009, available online from `http://arxiv.org/abs/0903.0096v2`.

[5] G. Bianchi, "Performance Analysis of the IEEE 802.11 Distributed Coordination Function," *IEEE Journal on Selected Areas in Communications*, vol. 18, no. 3, pp. 535–547, March 2000.

[6] A. Kumar, E. Altman, D. Miorandi, and M. Goyal, "New insights from a fixed point analysis of single cell IEEE 802.11 WLANs," *IEEE/ACM Transactions on Networking*, vol. 15, no. 3, pp. 588–601, June 2007, also appeared in INFOCOM 2005.

[7] R. Boorstyn, A. Kershenbaum, B. Maglaris, and V. Sahin, "Throughput Analysis in Multihop CSMA Packet Radio Networks," *IEEE Transactions on Communications*, vol. 35, no. 3, pp. 267–274, March 1987.

[8] X. Wang and K. Kar, "Throughput Modeling and Fairness Issues in CSMA/CA Based Ad Hoc Networks," in *IEEE INFOCOM*, 2005.

[9] M. Garetto, T. Salonidis, and E. W. Knightly, "Modeling Per-flow Throughput and Capturing Starvation in CSMA Multi-hop Networks," *IEEE/ACM Transactions on Networking*, to appear, Also appeared in INFOCOM 2006.

[10] M. Durvy, O. Dousse, and P. Thiran, "Border Effects, Fairness, and Phase Transitions in Large Wireless Networks," in *INFOCOM'08*.

[11] H. Q. Nguyen, F. Baccelli, and D. Kofman, "A Stochastic Geometry Analysis of Dense IEEE 802.11 Networks," in *IEEE INFOCOM'07*.

[12] T. Bonald, A. Ibrahim, and J. Roberts, "Traffic Capacity of Multi-Cell WLANs," in *ACM SIGMETRICS'08*.

[13] A. Kershenbaum, R. R. Boorstyn, and M.-S. Chen, "An Algorithm for Evaluation of Throughput in Multihop Packet Radio Networks with Complex Topologies," *IEEE Journal on Selected Areas in Communications*, vol. SAC-5, no. 6, pp. 1003–1012, July 1987.

[14] K. K. Leung and B.-J. J. Kim, "Frequency Assignment for Multi-Cell IEEE 802.11 Wireless Networks," in *Proceedings of VTC'2003*.

[15] A. Mishra, V. Brik, S. Banerjee, and A. S. W. Arbaugh, "A Client-driven Approach for Channel Management in Wireless LANs," in *IEEE INFOCOM'06*, 2006.

[16] A. Mishra, V. Shrivastava, D. Agrawal, S. Banerjee, and S. Ganguly, "Distributed channel management in uncoordinated wireless environments," in *ACM Mobicom'06*, 2006, pp. 170–181.

[17] D. J. Leith and P. Clifford, "A Self-Managed Distributed Channel Selection Algorithm for WLANs," in *Proceedings of RAWNET'06*.

[18] B. Kauffmann, F. Baccelli, and A. Chaintreau, "Measurement-Based Self Organization of Interfering 802.11 Wireless Access Networks," in *IEEE INFOCOM'07*, 2007.

[19] F. P. Kelly, *Reversibility in Stochastic Networks*. John Wiley, 1979.

[20] S. McCanne and S. Floyd., "The ns Network Simulator." http://www.isi.edu/nsnam/ns/.

[21] P. S. Sastry, V. V. Phansalkar, and M. A. L. Thathachar, "Decentralized Learning of Nash Equilibria in Multi-Person Stochastic Games With Incomplete Information," *IEEE Transactions on Systems, Man, and Cybernetics*, vol. 24, no. 5, pp. 769–777, 1994.